Available online at www.sciencedirect.com
SCIENCE DIRECT
Journal of Catalysis 227 (2004) 375–383
JOURNAL OF CATALYSIS
www.elsevier.com/locate/jcat

Isopropylation of benzene catalyzed by H/β zeolite catalysts with different crystallinities

M.W. Kasture, P.S. Niphadkar, N. Sharanappa, S.P. Mirajkar, V.V. Bokade, P.N. Joshi *

Catalysis Division, National Chemical Laboratory, Pune 411 008, India

Received 3 June 2004; revised 23 July 2004; accepted 26 July 2004

Available online 3 September 2004

Abstract

The protonic forms of zeolite beta (H/β) with different crystallinities were obtained by postsynthesis modification of phases that were obtained by varying crystallization periods during progressive crystallization from a $(TEA)_2O$–Na_2O–SiO_2–Al_2O_3–H_2O system at 413 K. These catalytic materials were characterized using powder X-ray diffraction, ^{27}Al MAS NMR, nitrogen adsorption, temperature-programmed ammonia desorption (TPAD), sorption of benzene probe molecules, and chemical composition. Evaluation of the catalysts for isopropylation of benzene reaction using isopropanol as alkylating agent was carried out in a continuous, down–flow, fixed-bed reactor at 483 K, liquid hour space velocity (LHSV) of 2.5 h^{-1}, and feed (isopropanol: benzene) molar ratios ranging from 1:6.5 to 4:6.5. The effect of time on stream on the benzene conversion and cumene selectivity was also studied. The pore volume accessible to benzene in catalyst was found to provide a more realistic measure for screening the catalyst as compared to percentage XRD crystallinity. A catalyst, which is XRD amorphous in nature, has exhibited nearly 27% benzene conversion and 48% cumene selectivity when compared with fully crystalline catalyst. Cumene selectivity was found to increase with increase in time on stream when the feed used contained a IPA/benzene molar ratio below 0.31. The number of strong Brönsted acid sites was found to increase with the increase in the crystallinity up to 85% XRD crystallinity. Above 85% XRD crystallinity, no considerable improvement was observed in catalyst activity as far as benzene conversion and cumene selectivity are concerned.

Keywords: Zeolite beta; Crystallinity; Characterization; Benzene isopropylation; Cumene; Acidity

1. Introduction

Hydrothermal crystallization of zeolite beta from aluminosilicate gel is a very complex process. The crystallization period is one of most important parameters that governs the kinetics of nucleation and crystal growth of the zeolitic phase. Pure and fully crystalline zeolite beta was found to be a suitable catalyst for the cracking of paraffins [1], isomerization of *n*-heptane [2] and *n*-hexane [3], and for the disproportionation and transalkylation of toluene and C_9 aromatics [4,5]. The efficiency of the zeolite beta as a catalyst is mostly related to its well-defined crystalline structure that leads to shape-selective catalysis occurring within the micropore system. The control of the crystallinity during the pathway of the crystallization process is crucial for monitoring adequately the activity and selectivity of the catalyst. The influence of various parameters such as gel composition, nucleation, temperature, and reaction time on the synthesis of zeolite beta under hydrothermal conditions has been well documented [6–8]. Among ion-exchanged forms of zeolite beta, the protonic form was found to possess the highest acidity [9].

Isopropyl benzene or cumene is an important industrial intermediate for the production of phenol. The processes based on the use of Friedel–Crafts catalysts [10] or solid phosphoric acid [11] catalysts suffer substantially from the drawbacks deriving from corrosion and environmental problems. To minimize these drawbacks, a variety of solid catalysts, especially zeolites, have been studied for this reaction

* Corresponding author. Fax: +91 20 25890976.
E-mail address: joshi@cata.ncl.res.in (P.N. Joshi).

0021-9517/$ – see front matter
doi:10.1016/j.jcat.2004.07.028

[12–15]. Zeolite beta has been proven to be a potential catalyst on account of its high activity, selectivity, and stability, under both liquid and vapor phase conditions [15–19]. The parameters such as Si/Al ratio, isomorphous substitution, alkylating agent, temperature, space velocity, and reactant mole ratios are reported for alterations in the product selectivity [20,21]. The influence of yet another important parameter, viz. the percentage crystallinity of zeolite beta on catalytic behavior in cumene synthesis, has not received any attention in previous publications. However, ZSM-5 zeolite-based aluminosilicate samples of low crystallinity have been reported [22] to exhibit higher selectivity and yield in skeleton isomerization of linear butenes.

The objective of the work described here was to investigate the catalytic behavior of the protonic forms of zeolite beta (H/β) catalysts with different crystallinities in the commercially important isopropylation of benzene reaction. H/β catalysts with different crystallinities were obtained by post-synthesis modification of the phases that were obtained by varying the crystallization period during progressive crystallization from a $(TEA)_2O$–Na_2O–SiO_2–Al_2O_3–H_2O system at 413 K. The samples were characterized for percentage crystallinity, nature of aluminic species, surface area, acidity, benzene uptake capacity, and chemical composition.

2. Experimental

2.1. Catalyst synthesis and characterization

All the samples used in this work were crystallized under hydrothermal conditions from the aluminosilicate gel having an oxide molar composition 6.0 $(TEA)_2O$:2.4 Na_2O:30.0 SiO_2:Al_2O_3:840.0 H_2O. The reagents used were sodium aluminate (43.8% Al_2O_3, 39.0% Na_2O), silica sol (40% SiO_2), tetraethylammonium hydroxide (TEAOH, aq. 30% wt/wt solution), sodium hydroxide (AR), and deionized water. In order to obtain the samples with different crystallinities, the kinetics of crystallization was carried out under static conditions at 413 K. The final homogeneous reaction mixture was distributed into several stainless-steel autoclaves, which after being sealed were placed in an air-heated oven maintained at 413 K. After reaching the crystallization temperature, the autoclaves were taken out of the oven one by one and quenched to room temperature and thus the extent of crystallization as a function of crystallization period was monitored. The solid products were separated by centrifugation, washed thoroughly with deionized water, and then dried at 393 K in a static air oven for 12 h. The dried products obtained after crystallization periods of 17, 37, 54, 63, and 72 h were designated as A, B, C, D, and E, respectively. These samples were then calcined at 823 K for 10 h under flowing air. The temperature was increased from room temperature to 823 K with rate of 1 K/min. The calcined sample thus obtained was further subjected for repetitive ion exchange using 1 M ammonium chloride solution (in the proportion 15 ml per gram of solid) for 3 times at 343 K for 6 h. Excess salt was washed by deionized water until there was no detectable chloride ions and the solid was dried at 393 K. These samples were further subjected to calcination at 773 K for 6 h under flowing air for converting them into corresponding protonic forms and designated as Cat A, Cat B, Cat C, Cat D, and Cat E.

The phase purity and crystallinity of the samples obtained at different intervals of time were determined by powder X-ray diffraction (Rigaku D Max III VC, Japan) using Ni-filtered Cu$K\alpha$ radiation. After background subtraction, the sum of the areas under the five characteristic peaks of zeolite beta in the 2θ range of 6.44–9.44, 19.32–24.42, 26.30–27.52, 32.72–34.16, and 42.84–44.82 was taken as a measure of crystallinity, by comparison to a most crystalline and pure beta phase, sample E, obtained in the present study. ^{27}Al MAS NMR spectra were obtained on a Bruker MSL-300 NMR spectrometer at 78.2 MHz with 3.0 kHz spinning speed, 1.5 μs excitation pulses (solution $\pi/2 = 9$ μs), and 0.25 s recycle times. Chemical shifts were referred to external $Al(H_2O)_6^{3+}$ in aqueous $AlCl_3$ solution. Low temperature nitrogen adsorption was carried out using Omnisorp, 100 CX. Benzene sorption was carried out using an all-glass apparatus at 298 K. The sample was activated at 623 K under vacuum (10^{-6} Torr) and then it was cooled down to 298 K. The vapors of liquid benzene at a relative pressure of 0.5 were allowed to contact with the activated sample for 2 h. and weight gain was measured with the help of a cathetometer. The chemical composition of the samples was established by determining the silicon and aluminum content by combination of wet chemical and atomic absorption (Hitachi Z-8000) methods. Temperature-programmed ammonia desorption (TPAD) was performed on protonic forms using a Micromeritics AutoChem 2910 (USA). The amount of 0.1 g of sample was loaded and activated at 773 K, in a quartz cell, in He flow (20 ml/min) for the period of 2 h. Presaturation was accomplished by passing 10% ammonia in He for 1 h at ambient temperature. Then the sample was flushed with He for 1 h at 373 K to remove excess ammonia. The adsorbed ammonia was desorbed in He flow (30 ml/min) with a heating rate of 10 K/min and the temperature was raised from 373 K to 773 K. The desorbed ammonia was detected by TCD. The TPAD profile was subjected for deconvolution using Gaussian lineshapes for quantitative estimation.

2.2. Catalyst performance

Isopropylation of benzene over protonic forms of beta zeolite samples with different crystallinities was carried out in a continuous, down–flow, fixed bed reactor at atmospheric pressure. The amount of 2.0 g of 10–20 mesh granules of self-bonded catalyst was loaded in the reactor. Before the start of the reaction run, the catalyst was activated at 723 K for 8 h in air to drive off moisture and adsorbed hydrocarbon, if any. Reactants (benzene and isopropyl alcohol) were fed through a syringe pump (ISCO, USA) into the reactor at

the desired reaction temperature. The analytical grade benzene and isopropyl alcohol (E.Merck India Ltd.) were used in this study. The products were analysed in a Shimadzu gas chromatograph (Model GC 15A), fitted with an Apiezome L (B.P. 1/1) column, using a flame ionization detector. The column employed was of 0.0032 m i.d. ×50 m length. The conversion of benzene and cumene yield as a function of time on stream over H/beta catalysts was investigated at 483 K with liquid hour space velocity (LHSV) of 2.5 h^{-1} and feed (isopropanol:benzene) molar ratios ranging from 1:6.5 to 4:6.5. Quantification of various products was accomplished using response factors of typical standard mixtures and the liquid mass balance was of the order of 98%.

3. Results and discussion

3.1. Characterization

3.1.1. Powder X-ray diffraction

From several synthesis runs, samples were selected on the basis of different crystallinities. Fig. 1 shows the progressive development of the nature of the phases at different crystallization periods and in turn of different crystallinities. The powder XRD pattern of sample A has shown an amorphous nature and hence it was assigned to 0% crystallinity. Characteristic peaks of zeolite beta start appearing after 17 h and the fully crystalline pure beta zeolitic phase is obtained at 72 h (sample E), which was assigned as 100% crystallinity. The intermediate samples B, C, and D have shown 31, 67, and 85% crystallinity, respectively. Crystallization kinetics curve (Fig. 1, inset) exhibited a sigmoidal or S-type nature, indicating different rates of crystallization at different crystallization periods. Moreover, the rate of crystallization was found to decrease as the crystallization process approaches completion, indicated by constancy, i.e., 100% crystallinity. The powder XRD pattern of sample E matches well with the reported one [8], confirming the well-crystalline zeolite beta phase with no other impurity. The powder XRD patterns of the samples before and after postsynthesis modifications such as calcination, ion exchange followed by calcination showed identical profiles, indicating no phase change or structural damage. Although, some alterations in the relative peak intensities were observed, there were hardly any difference in the peak positions and percentage crystallinity values. Thus any postsynthesis treatment has not affected the percentage crystallinity as well as the phase purity.

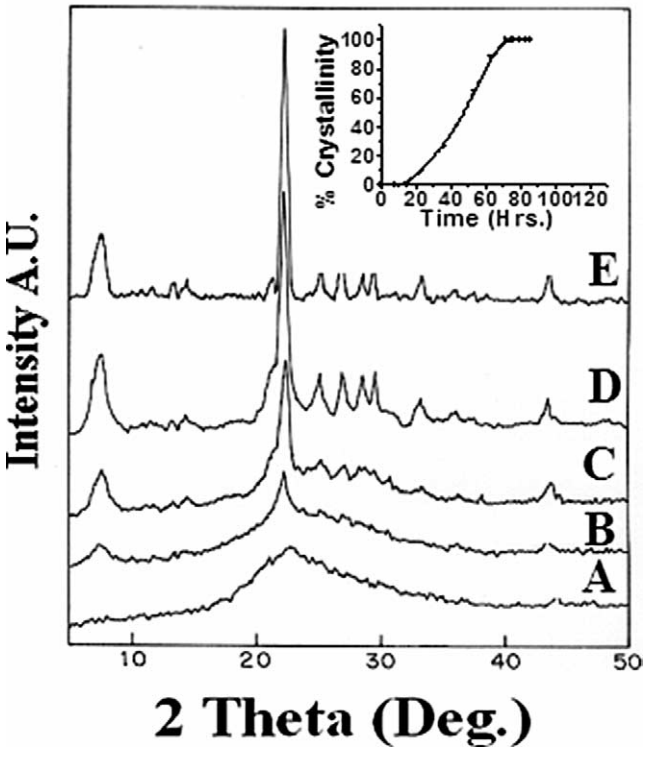

Fig. 1. Powder X-ray patterns of as-prepared zeolite beta phases obtained during hydrothermal crystallization. (Inset: Kinetics of crystallization at 413 K.)

3.1.2. ^{27}Al MAS NMR

^{27}Al MAS NMR spectra of different H/β samples are shown in Fig. 2. All the samples have exhibited a peak about 50 ppm assigned to tetrahedral aluminum. The absence of a signal (around zero ppm) due to octahedrally coordinated aluminum species confirms the fact that there is neither dealumination from the crystalline framework occurring during postsynthesis modification nor any octahedral aluminic species present in all the samples under investigations. However, the extent of broadening of NMR lines was found to decrease with the increase in the crystallinity, suggesting reduced distribution of aluminum with atoms having lower average coordination symmetry [23].

3.1.3. Compositional, textural, and sorptive characteristics

Table 1 shows the evolution of the SiO_2 and Al_2O_3 content and in turn SiO_2/Al_2O_3 molar ratio in the solids as a

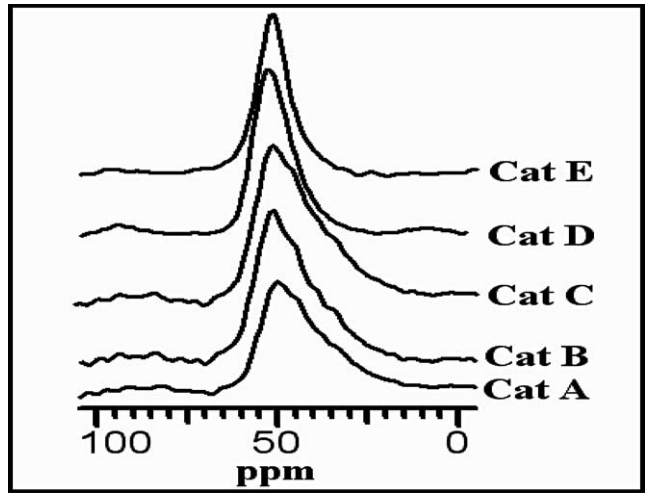

Fig. 2. ^{27}Al MAS NMR spectra of H/β samples with different crystallinities.

Table 1
Compositional, textural, and sorptive properties of H/β catalysts

Sample designation	Powder XRD crystallinity (%)	Chemical analysis (on dry basis)			N_2 adsorption[a]	Benzene sorption[b]
		SiO_2 (wt%)	Al_2O_3 (wt%)	SiO_2/Al_2O_3 molar ratio	micropore surface area (m^2/g)	uptake (mmol g^{-1})
Cat A	0	94.30	5.61	28.58	62.23	0.4
Cat B	31	94.35	5.56	28.81	270.00	0.9
Cat C	67	94.44	5.49	29.20	428.00	1.8
Cat D	85	94.59	5.36	29.95	486.00	2.2
Cat E	100	94.61	5.29	30.38	536.00	2.4

[a] Low-temperature (78 K) nitrogen adsorption data; activation temperature, 623 K.
[b] Temperature = 298 K, $P/P_o = 0.5$ ($P_o = 95.2$ Torr), time = 2 h.

function of the degree of the crystallinity. It clearly indicates that the SiO_2/Al_2O_3 molar ratio in the product increases with the increase in the crystallinity. Since the chemical analysis of mother liquor has not shown any contribution of aluminum, most of the aluminum was found to be located in the recovered X-ray amorphous solid of whose SiO_2/Al_2O_3 molar ratio was 28.58. Moreover, all the aluminum was in the tetrahedral coordination as indicated by ^{27}Al MAS NMR. Upon progressive crystallization, solids were found to become more and more siliceous. It is difficult to correlate the SiO_2/Al_2O_3 molar ratio in the crystals to that of the solid as partly crystalline solids contain both the amorphous material and the zeolite beta crystals. The micropore surface area obtained from low-temperature nitrogen adsorption data was also found to increase in nonlinear fashion with the increase in percentage crystallinity. It is interesting to note that the XRD amorphous sample has shown a micropore surface area of the order of 62.28 m^2/g, which is around 12% of that of fully crystalline samples. Probably, the presence of crystals of zeolite beta that have a much smaller size and below the XRD detection limit may be contributing to the micropore surface area observed for Cat A. The benzene uptake capacity for different H/β catalysts was estimated, as benzene is the feed molecule for probing the catalytic performance of these catalysts. It can be seen from Table 1 that, there is a concurrence between the crystallinity and the equilibrium benzene sorption capacity. The pore volume of Cat E calculated from the equilibrium benzene uptake capacity matches well with that of reported data in the literature [6,24].

3.1.4. Temperature-programmed ammonia desorption

The variation in the number and distribution of the acid sites as a function of crystallinity was estimated by TPAD. Fig. 3 illustrates the TPAD curves for all H/β catalysts. After deconvolution, two desorption peaks were classified as weak and strong acid sites according to lower and higher temperatures of the peak maximum, respectively. Since the low-temperature peak was ascribed to the desorption of weakly held ammonia from nonacid sites and distinct long tailing desorption of ammonia at temperatures higher than 600 K is a characteristic of beta zeolite [25], the high-temperature peak that corresponds to strong Brönsted acid sites (–OH of the framework aluminum atoms) was considered for examining the relation between crystallinity and number of strong Brönsted acid sites. Fig. 3, inset, depicts the relationship observed between number of strong Brönsted acid sites and percentage XRD crystallinity. The XRD amorphous sample has exhibited few Brönsted acid sites (6.5% of fully crystalline sample) indicative of the presence of small zeolite beta crystals that are below the XRD detection limit. It is interesting to note that, even though the solid becomes more and more siliceous with increase in the crystallinity, the number of Brönsted acid sites increases up to 85% crystallinity. This suggests that progressive incorporation of the aluminum in the framework takes place during the crystallization process up to 85% crystallinity. Moreover, the rate of incorporation of silicon in the framework seems to be higher than that of aluminum. In addition to this, the leveling off of number of Brönsted acid sites at crystallinity values higher than 85% indicates that further increases in the crystallinity may be due to incorporation of silicon only in the framework resulting in a silica-rich surface.

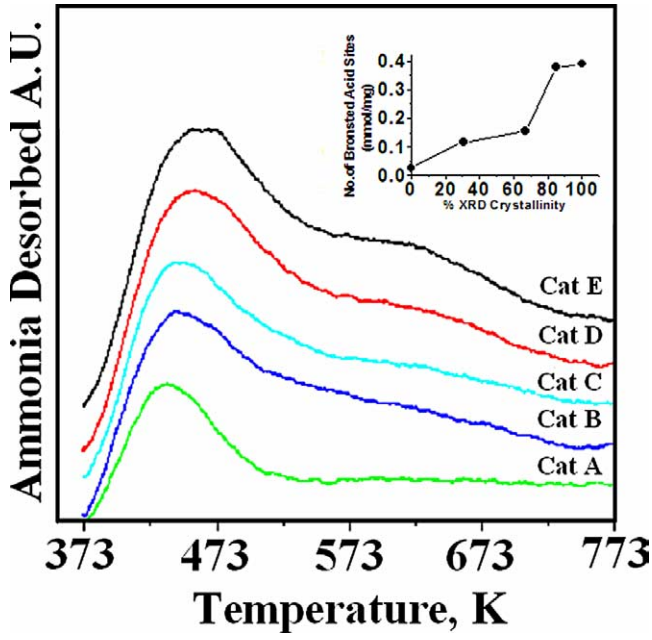

Fig. 3. TPAD profiles of H/β catalysts with different crystallinities. (Inset: Relationship between number of strong Brönsted acid sites and percentage XRD crystallinity.)

3.2. The catalytic behavior of H/β zeolite catalysts with different crystallinities

The alkylation of benzene with isopropanol is known [26] to proceed through the dehydration of an alcohol to alkene formation and the alkene reacts via a carbonium ion mechanism with gas-phase benzene or cumene to produce cumene and/or diisopropylbenzene (DIPB), respectively. In this reaction, in addition to the alkylation, other undesired reactions such as isomerization, cracking, and disproportionation of alkyl aromatics also occur, resulting in the formation of compounds such as toluene and C_8–C_{11} aromatics [20,21]. Due to presence of such products formed by secondary reaction in the locus of the reaction pathway, the yield of desired product drops considerably, depending upon the reaction conditions and characteristics of the catalysts.

3.2.1. Catalyst screening

The influence of the percentage XRD crystallinity of H/β catalysts on the product distribution in the alkylation of benzene with isopropanol was investigated under an identical set of reaction conditions. The results obtained after 4 h time on stream are summarized in Table 2. All the catalysts have shown propylene (C_3) conversion more than 98%, indicating propylene conversion is independent of the catalyst crystallinity mainly because of the formation of propylene via dehydration of isopropanol that is occurring at 483 K prior to reacting with benzene [26]. Therefore, the results are discussed on the basis of benzene conversion. It is clearly evident from Table 2 that, the characteristics of the catalytic materials govern the extent of the desired and undesired reactions leading to the formation of different products in different concentration. Cat A has shown the formation of aliphatics in high concentration as compared to other catalysts. Moreover, other products (desired and undesired) are formed in lower concentrations. Thus, higher propylene conversion and lower conversion of benzene over Cat A seems to be responsible for the formation of aliphatics in higher concentrations. The benzene conversion was found to follow the trend Cat E ≅ Cat D > Cat C > Cat B > Cat A. Cat A has exhibited 5.43% benzene conversion and 42.82% cumene selectivity. By a comparison to Cat E, these values of benzene conversion and cumene selectivity amount nearly to 27 and 48%, respectively. In order to examine the typical catalytic behavior of Cat A, another XRD amorphous material was obtained by following the same procedure except autoclaving and hydrothermal crystallization thereafter. This sample was found to be completely inactive under the same reaction conditions. Thus, it can be concluded that much smaller size crystals of zeolite beta, which are below the XRD detection limit, may be present in Cat A.

The cumene selectivity was found to follow the same trend as benzene conversion. The leveling off of cumene selectivity at crystallinity values higher than 85% indicates that a further increase in the crystallinity has no considerable effect on either benzene conversion or cumene formation

The concentration of compounds such as toluene and C_8 aromatics that are formed by the occurrence of secondary reactions [21] was found to decrease with the increase in crystallinity of the catalyst. Since the improvement in the crystallinity is associated with the changes in other properties such as micropore surface area, pore volume, framework composition, nature of aluminic species, and acidity, the cumulative effect of these properties is believed to suppress other side reaction by reacting propylene with benzene in one step (fast reaction regime), leaving little opportunity for further isomerization or cracking or disproportionation reactions.

Even though, all the catalysts have shown the formation of *n*-propylbenzene less than 0.5 wt%, a marginal but increasing trend in the formation of *n*-propylbenzene with increase in crystallinity was observed. Thus, it seems that the formation of *n*-propylbenzene by isomerization of cumene formed might be occurring due to higher contact time (lower LHSV of 2.5 h^{-1}) [20] and in particular the extent of its formation depends on the characteristics of the catalyst and the level of cumene formation.

The C_{10-11} aromatics are formed by the alkylation of benzene with C_4 alkenes that are produced from the reaction of isopropanol over acidic zeolites [27]. The decreasing trend observed in the formation of C_{10-11} aromatics with increasing crystallinity suggests that the rate of reaction to-

Table 2
Performance comparison of catalysts for benzene isopropylation reaction

Product composition (wt%)	Cat A	Cat B	Cat C	Cat D	Cat E
Aliphatics	1.85	0.16	0.15	0.17	0.17
Benzene	89.14	82.00	79.30	76.00	75.30
Cumene	4.65	13.93	17.41	21.25	21.82
Toluene + C_8 aromatics	3.02	2.56	1.40	0.82	0.85
n-Propylbenzene	–	0.05	0.10	0.13	0.20
C_{10-11} aromatics	0.39	0.34	0.29	0.15	0.09
DIPB	0.95	1.00	1.38	1.51	1.61
Performance					
C_3 conversion (%)	98.15	99.84	99.85	99.83	99.83
Benzene conversion (%)	5.43	13.00	15.90	19.40	20.15
Cumene selectivity (%)	42.82	77.40	84.00	88.54	88.34

Reaction conditions: Temperature, 483 K; feed molar (isopropanol:benzene) ratio, 1:6.5; LHSV = 2.5 h^{-1}. Time on stream, 4 h.

ward desired product increases with reduction in C_4 alkene formation. The increased formation of DIPB with increase in crystallinity may be attributed to the higher rate of alkylation of cumene as compared to rate of alkylation of benzene and/or transalkylation reaction [20] on account of increasing total acidity of the catalysts.

Since Cat A was found to be catalytically active to some extent, an attempt was made to compare the catalytic behavior of the catalysts with different crystallinities as a function of pore volume accessible to benzene instead of XRD crystallinity. A comparison of pore volume calculated on the basis of benzene uptake capacity with percentage crystallinity estimated from X-ray powder diffraction data is presented in Fig. 4 (inset). Though, a linear relationship was observed between pore volume and percentage XRD crystallinity, the pore volume that is accessible to benzene molecules in Cat A was nearly 16% of the pore volume of Cat E. This again supports the presence of X-ray amorphous zeolitic material in Cat A. If it is assumed that the extent of adsorption of benzene depends on the number and/or extent of negative charge of the framework oxygen atoms in the unit cell, the increase in crystallinity might result in more numbers of negative charges or higher negative charge on the oxygen atoms resulting in a greater interaction of hydrogen atoms of benzene molecules with accessible oxygen atoms. Thus, we believe that benzene uptake capacity is a powerful tool for evaluating the crystallinity and in turn the catalytic performance of these catalytic materials. In view of the above, the catalytic behavior of these catalysts was compared with the pore volume accessible to the benzene of freshly activated sample. Such correlation has been depicted in Fig. 4. Both the benzene conversion and cumene selectivity were observed to be increased with the increase in pore volume up to 0.18 ml/g of the catalyst. Further increase in the pore volume has not shown considerable increase in either benzene conversion or cumene selectivity. However, the deviation from the linearity of both the correlations and with each other may partly be attributed to other characteristics such as acidity, framework composition, and to some extent amount and nature of amorphous material present in the catalysts. Prompted by the above observations, the influence of other reaction parameters such as reactant mole ratio and time on stream on benzene conversion and cumene selectivity was studied over H-beta catalysts with different crystallinities.

3.2.2. *Effect of IPA: benzene mole ratio*

One of the typical ways of monitoring conversions and selectivities is to vary the mole ratio of reactants. The influence of isopropanol (IPA) to benzene mole ratio on benzene conversion and cumene selectivity was investigated by varying the IPA/benzene mole ratio in the range of 0.154 to 0.615 [IPA:benzene = 1:6.5 to 4:6.5]. Two extreme catalysts were chosen for this study, viz. Cat A and Cat E. Fig. 5 illustrates the relationship between benzene conversion and cumene selectivity with the time on stream for both catalysts. The effect of IPA/benzene mole ratio on the benzene conversion and cumene selectivity over Cat A is represented in Figs. 5a and b, respectively. It is clearly evident from Fig. 5a that, by increasing isopropanol concentration in the feed keeping benzene concentration constant, Cat A exhibited a decreasing trend in the benzene conversion. This can be explained partly on the basis of lower pore volume and less available active surface area for the reaction. Since the formation of propylene via dehydration of isopropanol occurs at 483 K prior to reacting with benzene [26], the multilayer formation of propylene over the active catalyst surface area may cause reduction in the mass-transfer diffusional rate of benzene resulting in a drop in the rate of reaction of benzene with propylene. Similarly, the benzene conversion was found to decrease with increase in time on stream for all the mole ratios. However, the extent of decrease was found to depend on the reactant mole ratio. It is interesting to note that, despite showing higher benzene conversion with the use of feed having a lower IPA/benzene mole ratio, faster deactivation was observed with time on stream. Such decrease in the catalytic activity may be due to catalyst deactivation on account of the formation of heavy coke on the active surface of the catalyst. It is known [15,28] that fewer acid sites lead to the formation of more oligomers which are responsible for the coke formation. In the present case, since isopropanol is dehydrating to propylene/propene, it is likely that Cat A which has fewer acid sites may be deactivating fast on account of the formation of higher amounts of propylene/propene oligomers with increase in time on stream.

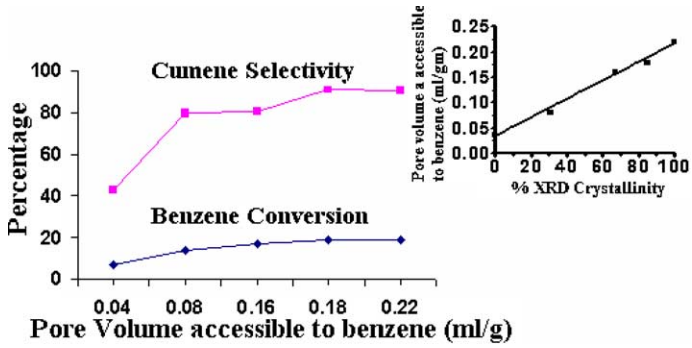

Fig. 4. Correlationship between catalytic performance and pore volume that is accessible to benzene of the H-beta catalyst with different crystallinities. (Inset: Relationship between pore volume accessible to benzene and XRD crystallinity.)

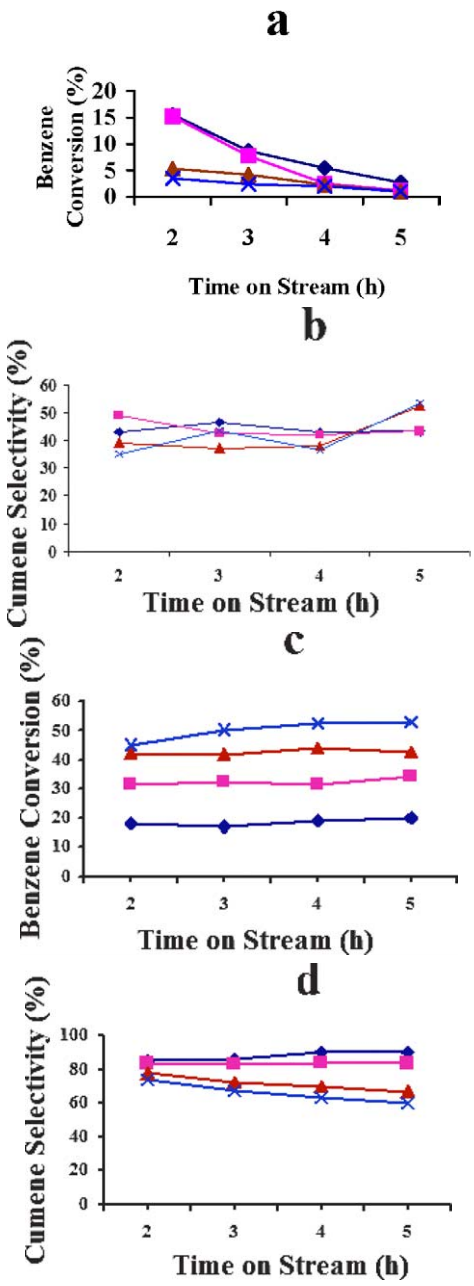

Fig. 5. Effect of reactant (IPA:benzene) mole ratio (◆) 1:6.5, (■) 2:6.5, (▲) 3:6.5, (X) 4:6.5 on (a) percentage benzene conversion over Cat A, (b) percentage cumene selectivity over Cat A, (c) percentage benzene conversion over Cat E, and (d) percentage cumene selectivity over Cat E.

This has also been reflected in the formation of aliphatics in higher concentrations as can be seen from Table 2.

The change in the cumene selectivity with change in isopropanol concentration over Cat A is represented in Fig. 5b. It can be seen from this figure that the lower the IPA/benzene mole ratio the better the stability of the cumene selectivity with time on stream. The abrupt variation in cumene selectivity was observed with higher IPA/benzene mole ratios.

The effect of IPA/benzene mole ratio on the benzene conversion and cumene selectivity over Cat E is represented in Figs. 5c and d, respectively. It can be seen clearly from Fig. 5c that the benzene conversion not only increases with the increase in IPA/benzene mole ratio but also with the time on stream for all the ratios. It is interesting to note that these trends are exactly opposite to those observed for Cat A. This reverse trend can be partly attributed to the higher pore volume and larger number of active centers on the larger surface area of Cat E. In order to examine the cause of the least deactivation of Cat E as compared to Cat A, the spent Cat A and Cat E were analyzed for carbon and hydrogen contents after running them for 5 h time on stream with feed containing an IPA/benzene mole ratio of 1:6.5. Spent Cat A has shown the contribution of 6.22% carbon and 2.37% hydrogen whereas Cat E has shown the presence of 0.86% carbon and 1.25% hydrogen. Thus, in case of Cat E, the minimized multilayer formation of propylene and formation of propylene/propene oligomers on the large active surface area seems to be responsible for the increased benzene conversion and life of the catalyst, respectively. As far as cumene selectivity is concerned, it is clearly seen from Fig. 5d that the lower the IPA/benzene mole ratio the higher the cumene selectivity. However, cumene selectivity was found to increase with increase in time on stream when the IPA/benzene mole ratio was below 0.31. The reverse trend was observed when the IPA/benzene mole ratio used was above 0.31. The decreased cumene selectivity is associated with the formation of the unwanted products, such as toluene, C_8 aromatics, *n*-propylbenzene, C_{10} aromatics, and DIPB. Thus, it seems that unwanted consecutive side reactions like isomerization, cracking, and disproportionation are favored when well crystalline catalysts and feed containing IPA/benzene mole ratios higher than 0.31 were used. When compared to Cat A, the cumene selectivity stability trend is more or less same only when lower IPA/benzene mole ratios are used. In view of above observations a reactant IPA:benzene mole ratio of 1:6.5 was used for the further screening the H-beta catalysts with wide range of crystallinity for their catalytic performance in cumene synthesis.

Thus, the influence of yet another reaction parameter, i.e., time on stream on benzene conversion and cumene selectivity was studied over H-beta catalysts with different crystallinities, keeping constant a reactant IPA: benzene mole ratio of 1: 6.5.

3.2.3. *Effect of time on stream*

In order to investigate the influence of XRD crystallinity of H/β catalysts on the catalytic activity as a function of time on stream, each catalyst was screened on stream for the period of 5 h under an identical set of reaction conditions. The product was collected after every hour. The variations observed in benzene conversion and cumene selectivity as a function of time on stream over these catalysts are represented in Figs. 6a and b, respectively. It can be seen from Fig. 6a that, benzene conversion was found to increase with the crystallinity up to 85%. However, there is no remarkable difference in benzene conversion above 85% of the crys-

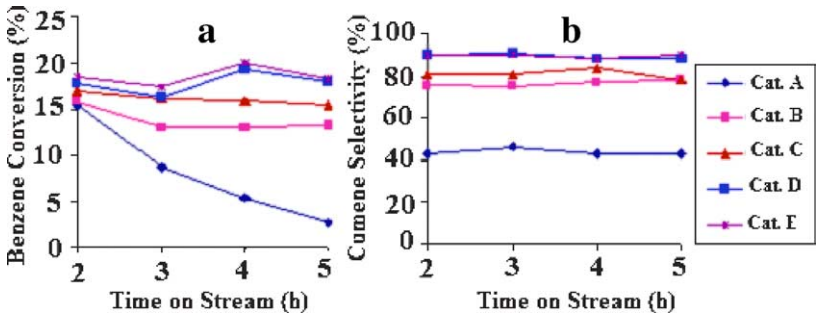

Fig. 6. Variations in (a) percentage benzene conversion and (b) percentage cumene selectivity as a function of time on stream over H-β catalysts with different crystallinities.

tallinity level. The increase in the benzene conversion with the increase in crystallinity up to 85% may partly be associated with an increase in the number of acidic sites, pore volume, and surface area. As far as the catalyst stability is concerned, except Cat A, most of the samples have shown similar trends. The cause for faster deactivation of Cat A has been discussed in earlier.

It can be clearly seen from Fig. 6b that, except Cat A, marginal variation in cumene selectivity was observed over the entire range of time on stream. Cat A has shown a decreasing trend in cumene selectivity as time progresses, suggesting faster deactivation compared to other candidates. The cumene selectivity of Cat B and C was found to be stabilized at around $80 \pm 4\%$, whereas for Cat D and E it was around $88 \pm 1\%$. The product distribution data tabulated in Table 2 and relevant discussion thereon can be treated as the basis for such variation in cumene selectivity as a function of crystallinity.

4. Conclusions

Catalysts with different crystallinities were prepared from a $(TEA)_2O$–Na_2O–SiO_2–Al_2O_3–H_2O system followed by their modification to protonic forms. These were characterized and their potentiality was investigated in benzene isopropylation reactions using isopropanol as alkylating agent. Progressive hydrothermal crystallization of zeolite beta has resulted into an increase in micropore surface area, bulk Si/Al ratio, and pore volume that is accessible to benzene molecules. No contribution of octahedral aluminic species was observed in protonic forms of zeolite beta, irrespective of their XRD crystallinity. The isopropyl alcohol conversion was observed to be more than 98%, irrespective of XRD crystallinity of the catalysts. When percentage XRD crystallinity was increased from 0 to 100, the percentage cumene selectivity was found to increase from 42.82 to 88.34, at the benzene conversion level from 5.43 to 20.15%. The smaller crystallites of zeolite beta below the XRD detection limit have shown a benzene conversion of 5.43% with cumene selectivity of 42.82%. Above 85% crystallinity, there is no considerable improvement in catalyst activity. The increase in the benzene conversion with the increase in crystallinity up to 85% may partly be associated with an increase in number of acidic sites, pore volume, and surface area. The feed containing an IPA/benzene molar ratio below 0.31 is the best fit for screening the H-β catalysts with a wide range of crystallinities for their catalytic performance in cumene synthesis. Unwanted consecutive side reactions, such as isomerization, cracking, and disproportionation, were found to be favored when well-crystalline catalysts and feed containing IPA/benzene mole ratios higher than 0.31 were used. The micropore surface area of the order 486 m^2/g and pore volume of the order of 0.18 cc/g of H-β catalyst were found to be the optimum values for the maximum benzene conversion and cumene selectivity as well. Except Cat A, marginal variation in cumene selectivity was observed over the entire range of time on stream. XRD amorphous material containing smaller crystallites of zeolite beta was found to be more sensitive for faster deactivation. Even though such materials may have a shorter pore length on account of which alkene should have a lower residence time within a zeolite pore environment, faster deactivation may partly be due to multilayer formation of propylene and formation of propylene/propene oligomers on the less active surface area.

Acknowledgments

The authors acknowledge the contributions of N.E. Jacob, R.K. Jha (nitrogen adsorption), and Violet Samuel (XRD). This work was partly funded by DST, New Delhi, India, and Dr. M.W.Kasture thanks DST for awarding a Young Scientist Fellowship.

References

[1] L. Boretto, M.A. Camblor, A. Corma, J. Perez-Pariente, Appl. Catal. 82 (1992) 37.
[2] J.K. Lee, H.K. Ree, Catal. Today 38 (1997) 235.
[3] Z.B. Wang, A. Kamo, T. Youeda, T. Komatsu, T. Yashima, Appl. Catal. 159 (1997) 119.
[4] J. Das, Y.S. Bhat, A.B. Halgeri, Catal. Lett. 23 (1994) 161.
[5] I. Wang, T.C. Tsai, S.T. Huang, Ind. Eng. Chem. Res. 29 (1990) 2005.
[6] J. Perez-Pariente, J.A. Martens, P.A. Jacobs, Zeolites 8 (1988) 46.
[7] M.A. Camblor, J. Perez-Pariente, Zeolites 11 (1991) 202.

[8] J. Perez-Pariente, J.A. Martens, P.A. Jacobs, Appl. Catal. 31 (1987) 35.
[9] K.S.N. Reddy, M.J. Eapen, H.S. Soni, V.P. Shiralkar, J. Phys. Chem. 96 (1992) 7923.
[10] H. Miki, US patent, 4,347,393 (1982) to Mitsui Petrochemical Industries, Ltd. (Tokyo, JP).
[11] E.K. Jones, D.D. Dettner, US patent, 2,860,173 (1958).
[12] W.W. Keading, R.F. Holland, J. Catal. 109 (1988) 212.
[13] E.S. Mortikov, S.R. Mirzabekova, A.G. Pogovelov, N.F. Konov, R.F. Merhanova, A.Z. Dorogochinskii, Kh.M. Minachev, Naftekhimiya 16 (1988) 701.
[14] A.R. Pradhan, B.S. Rao, V.P. Shiralkar, in: ZEOCAT 90 Conference, LipZig, GDR, August 20–23, 1990.
[15] G. Bellussi, G. Pazzuconi, C. Perego, G. Girotti, G. Terzoni, J. Catal. 157 (1995) 227.
[16] C.Y. Yeh, H.E. Barner, G.D. Suci, in: Garmisch-Partenkirchen (Ed.), Zeolites and Related Microporous Materials: State of the Art, vol. 84A, Elsevier, Amsterdam, 1994, p. 2311.
[17] A.V. Smirnov, F.D. Renzo, O.E. Lebedeva, D. Brunel, B. Chiche, A. Tavalro, B.V. Ramanovsky, in: H. Cou, et al. (Eds.), Progress in Zeolite and Microporous Materials, vol. 105B, Elsevier, Amsterdam, 1997, p. 1325.
[18] A.B. Halgeri, J. Das, Appl. Catal. A 181 (1999) 347.
[19] U. Sridevi, C.V.V. Satanarayan, B.S. Rao, N.C. Pradhan, B.K.B. Rao, V.V. Bokade, J. Mol. Catal. A: Chem. 181 (2002) 257.
[20] K.S.N. Reddy, B.S. Rao, V.P. Shiralkar, Appl. Catal. A 95 (1993) 53.
[21] A.R. Pradhan, A.N. Kotasthane, B.S. Rao, Appl. Catal. 72 (1991) 311.
[22] C.P. Nicolaides, Appl. Catal. A 185 (1999) 211.
[23] I. Kiricsi, C. Flego, G. Pazzuconi, W.O. Parker Jr., R. Millini, C. Perego, G. Bellusi, J. Phys. Chem. 98 (1994) 4627.
[24] R.L. Wadlinger, G.T. Kerr, E.J. Rosinski, US Patent 3,308,069 (1967) to Mobil Oil Corporation.
[25] Y. Miyamoto, N. Katada, M. Niwa, Micropor. Mesopor. Mater. 40 (2000) 271.
[26] J.R. Anderson, T. Mole, V. Christov, J. Catal. 61 (1980) 477.
[27] S.J. Kulkarni, S.B. Kulkarni, P. Ratnasamy, H. Hattori, K. Tanabe, Appl. Catal. 8 (1983) 43.
[28] S. Siffert, L. Gaillard, B.-L. Su, J. Mol. Catal. A: Chem. 153 (2000) 267.